Eur. Phys. J. B **52**, 469–476 (2006)
DOI: 10.1140/epjb/e2006-00326-3

THE EUROPEAN PHYSICAL JOURNAL B

Transport through a double barrier in Large Radius Carbon Nanotubes with a transverse magnetic field

S. Bellucci[1,a] and P. Onorato[1,2]

[1] INFN, Laboratori Nazionali di Frascati, P.O. Box 13, 00044 Frascati, Italy
[2] Department of Physics "A. Volta", University of Pavia, via Bassi 6, 27100 Pavia, Italy

Received 2 December 2005 / Received in final form 24 July 2006
Published online 21 August 2006 –

Abstract. We discuss the Luttinger Liquid behaviour of Large Radius Carbon Nanotube e.g. the Multi Wall ones (MWNT), under the action of a transverse magnetic field B. Our results imply a reduction with B in the value of the *bulk* critical exponent, α_{bulk}, for the tunneling density of states, which is in agreement with that observed in transport experiments. Then, the problem of transport through a Quantum Dot formed by two intramolecular tunneling barriers along the MWNT, weakly coupled to Tomonaga-Luttinger liquids is studied, including the action of a strong transverse magnetic field B. We predict the presence of some peaks in the conductance G versus B, related to the magnetic flux quantization in the ballistic regime, at a very low temperature T, and also at higher values of T, where the Luttinger behaviour dominates. The temperature dependence of the maximum G_{max} of the conductance peak according to the Sequential Tunneling follows a power law, $G \propto T^{\gamma_e - 1}$ with γ_e linearly dependent on the critical exponent, α_{end}, strongly reduced by B.

PACS. 05.60.Gg Quantum transport – 71.10.Pm Fermions in reduced dimensions – 73.63.-b Electronic transport in nanoscale materials and structures – 71.20.Tx Fullerenes and related materials; intercalation compounds

1 Introduction

In a recent paper [1] we discussed the transport through a double barrier for interacting quasi one-dimensional electrons in a Quantum Wire (QW), in the presence of a transverse magnetic field. Here we want to extend the results obtained there to an analogous device based on Large Radius Carbon Nanotubes (LRCN), such as the Multi Wall ones (MWNT). This aim is not trivial to pursue, because of the geometry-dependent electronic properties of the Carbon Nanotubes (CNs) and the effects of many subbands crossing the Fermi level in LRCNs.

Transport in 1 Dimension — Electronic correlations have been predicted to dominate the characteristic features in quasi one dimensional (1D) interacting electron systems. This property, commonly referred to as Tomonaga-Luttinger liquid (TLL) behaviour [2], has recently moved into the focus of attention by physicists, also because in recent years several electrical transport experiments for a variety of 1D devices, such as semiconductor quantum wires [3] (QWs) and carbon nanotubes (CNs) [4] have shown this behaviour.

In a 1D electron liquid Landau quasiparticles are unstable and the low-energy excitations take the form of plasmons (collective electron-hole pair modes): this is known as the breakdown of the Fermi liquid picture in 1D. The LL state has two main features: (i) the power-law dependence of physical quantities, such as the tunneling density of states (TDOS), as a function of energy or temperature; (ii) the spin-charge separation: an additional electron in the LL decays into decoupled spin and charge wave packets, with different velocities for charge and spin. It follows that 1D electron liquid are characterized by the power-law dependence of some physical quantities, as a function of the energy or the temperature. Thus, the tunneling conductance G reflects the power law dependence of the DOS in a small bias experiment [5]

$$G = dI/dV \propto T^{\alpha_{bulk}} \tag{1}$$

for $eV_b \ll k_B T$, where V_b is the bias voltage, T is the temperature and k_B is Boltzmann's constant.

The power-law behaviour characterizes also the thermal dependence of G when an impurity is present along the 1D devices. The theoretical approach to the presence of obstacles mixes two theories corresponding to the single particle scattering (by a potential barrier $V_B(\mathbf{r})$) and the TLL theory of interacting electrons. The single particle scattering gives the transmission probability, $|t|^2$, depending in general on the single particle energy ε. Hence,

[a] e-mail: bellucci@Inf.infn.it

following reference [6], the conductance, G, as a function of the temperature and $|t|$ can be obtained

$$G \propto |t(\varepsilon, T)|^2 \equiv |t(\varepsilon)|^2 T^{2\alpha_{end}}, \tag{2}$$

where we introduced a second critical exponent, α_{end}.

Intrinsic Quantum Dot — Experiments [7,8] show transport through an intrinsic quantum dot (IQD) formed by a double barrier within a 1D electron system, allowing for the study of the resonant or sequential tunneling. The linear conductance typically displays a sequence of peaks, when the gate voltage, V_g, increases. Thus, also the double-barrier problem has attracted a significant amount of attention among theorists [9–16], in particular the case of two identical, weakly scattering barriers at a distance d. In general, the transmission is non-zero for particular values of the parameters corresponding to a momentum k_F, such that $\cos(k_F d/2) = 0$. It follows that, although in a 1D electron system for repulsive interaction the conductance is suppressed at zero temperature by the presence of one impurity (a 1D metal becomes a perfect insulator), the presence of an IQD gives rise to some peaks in the conductance at $T = 0$ corresponding to the perfect transmission. This *resonant scattering* condition corresponds to an average particle number between the two barriers of the form $\nu + 1/2$, with integer ν, i.e. the "island" between the two barriers is in a degenerate state. If interactions between the electrons in the island are included, one can recover the physics of the Coulomb blockade [5,17].

The power-law behaviour characterizes also the thermal dependence of G in the presence of an IQD. A first theory about the transport through an IQD is known as *uncorrelated sequential tunneling* (UST), where an incoherent sequential tunneling is predicted. It follows the dependence of the peaks of the conductance according to the power law

$$G_{max} \propto T^{\alpha_{end}-1}.$$

Some experiments [7,8] showed transport through an IQD formed by a double barrier within a Single Wall CN (SWNT), allowing one to study the resonant or sequential tunneling. In order to explain the unconventional power-law dependencies in the measured transport properties of a CN, a mechanism was proposed [7,12], namely, *correlated sequential tunneling* (CST) through the island. The temperature dependence of the maximum G_{max} of the conductance peak, according to the CST theory, yields the power law behaviour

$$G_{max} \propto T^{\alpha_{end-end}-1} = T^{2\alpha_{end}-1}. \tag{3}$$

Recently a lot of theoretical work has been carried out on the double impurity problem in TLL systems. In an intermediate temperature range $\varepsilon_c \ll k_B T \ll \Delta_{dot}$, where ε_c is the Infra Red cut-off energy and Δ_{dot} is the level spacing of the dot, some authors [13,14] predict a behaviour according to the UST, while others [16] find results in agreement with the CST theory. In a recent paper [18] the authors discussed how the critical exponent can depend on the size of the dot and on the temperature, by identifying three different regimes, i.e. the UST at low T, a Kirchoff regime at intermediate T ($G_{max} \propto T^{2\alpha_{end}}$) and a third regime for $T \gg \Delta_{dot}$, with $G_{max} \propto T^{-1}$. Thus, in their calculations, obtained starting from spinless fermions on the lattice model, no evidence of CST is present.

Multi Wall Carbon Nanotubes — An ideal Single Wall CN (SWCN) is a hexagonal network of carbon atoms (graphene sheet) that has been rolled up, in order to make a cylinder with a radius about 1 nm and a length about 1 μm. The unique electronic properties of CNs are due to their diameter and chiral angle (helicity) [19]. MWCNs, instead, are made by several (typically 10) concentrically arranged graphene sheets with a radius above 5 nm and a length which ranges from 1 to some hundreds of μms. The transport measurements carried out in MWNTs reflect usually the electronic properties of the outer layer, to which the electrodes are attached. Thus, in what follows we mainly discuss the LRCNs as a general class of CNs including also MWNTs. In general the LRCNs are affected by the presence of doping, impurities, or disorder, what leads to the presence of a large number of subbands, N, at the Fermi level [20]. It follows that the critical exponent has a different form, with respect to that calculated in reference [1].

The bulk critical exponent can be calculated in several different ways, e.g. see reference [21] where we obtained

$$\alpha_{bulk} \approx \frac{1}{4N}\left(K_N + \frac{1}{K_N} - 2\right), \tag{4}$$

where

$$\frac{1}{K_N} \approx \sqrt{1 + \frac{N U_0(q_c, B)}{(2\pi v_F)}}.$$

Here v_F is the Fermi velocity, $U_0(p)$ corresponds to the Fourier transform of the 1D electron-electron interaction potential and $q_c = 2\pi/L$ is the infra-red natural cut-off due to the length of the CN, L. For a strictly 1D system, such as a CN in absence of magnetic field, $U_0(p)$ does not depend on the momenta of the interacting electrons. In general [22] we need to introduce two different couplings for two different forward scattering processes (with a small transferred momentum). The first term, g_2, is obtained by considering 2 scattered electrons with opposite momenta ($\pm k_F$). The second term, g_4, is obtained by considering 2 scattered electrons with (almost) equal momenta ($k_1 \sim k_2 \sim k_F$). It follows that

$$K_N \approx \sqrt{\frac{2\pi v_F + N\,(g_4 - g_2)\,/2}{2\pi v_F + N\,(g_4 + g_2)\,/2}},$$

which corresponds to the previous formula when $g_2 = g_4 = U_0(q_c)$. As in reference [22], the presence of a magnetic field gives $g_2 \neq g_4$ because of the edge localization of the currents with opposite chiralities, and we need the B dependent values of g_2 and g_4.

The value of α_{bulk} obtained in reference [21] is in agreement with the one obtained in reference [23], where also the end critical exponent was obtained as

$$\alpha_{end} \approx \frac{1}{2N}\left(\frac{1}{K_N} - 1\right). \tag{5}$$

Power law in MWNTs — One of the most significant observations made in the MWNTs has been the power-law behavior of the tunneling conductance as a function of the temperature or the bias voltage. The measurements carried out in MWNTs displayed a power-law behavior of the tunneling conductance, that gives a measure of the low-energy density of states. Also if the power law behaviour in the temperature dependence of G usually characterizes a small range of temperature (from some $-K$ up to some tens, rarely up to the room T), this behaviour allowed the measurements of the critical exponents α_{Bulk} ranging, in MWNTs, from 0.24 to 0.37 [24]. These values are, on the average, below those measured in the single-walled nanotubes, which are typically about 0.35 [25]. A similar behaviour was satisfactorily explained [21] in terms of the number of subbands by applying equation (4).

CNs under a transverse magnetic field — The effects of a transverse magnetic field B, acting on CNs were also investigated in past years. Theoretically, it is predicted that a perpendicular B field modifies the DOS of a CN [26], leading to the Landau level formation. This effect was observed in a MWNT single-electron transistor [27]. In a recent letter Kanda et al. [28] examined the dependence of G on perpendicular B fields in MWNTs. They found that, in most cases, G is smaller for higher magnetic fields, while α_{Bulk} is reduced by a factor 1/3 to 1/10, for B ranging from 0 to 4 T. Recently we discussed the effects of a transverse magnetic field in QWs [1] and large radius CNs [29]. The presence of $B \neq 0$ produces the rescaling of all repulsive terms of the interaction between electrons, with a strong reduction of the backward scattering, due to the edge localization of the electrons. Our results imply a variation with B in the value of α_{Bulk}, which is in fair agreement with the value observed in transport experiments [28].

Impurities, buckles and Intrinsic Quantum Dots — The magnetically induced localization of the electrons should have some interesting effects also on the backward scattering, owing to the presence of one or more obstacles along the LRCN, and hence on the corresponding conductance, G [1]. Thus, the main focus of our paper is the analysis of the presence of two barriers along a LRCN, at a fixed distance d. A similar device was realized by the manipulating individual nanotubes with an atomic force microscope which allowed one to obtain intratube buckles acting as tunneling barriers [7]. The SWNTs with two intramolecular buckles have been reported to behave as room-temperature single electron transistors. The linear conductance typically displays a sequence of peaks when the gate voltage, V_g, increases. The one-dimensional nature of the correlated electrons is responsible for the differences, with respect to the usual quantum Coulomb blockade theory.

We predict that, in the presence of a transverse magnetic field, a LRCN should show some oscillations in the conductance as a function of the magnetic field, analogous to those discussed in reference [1].

Summary — In this paper we want to discuss the issues mentioned above. In order to do so, we follow the same line of reasoning of our previous paper [1]

In Section 2 we introduce a theoretical model which can describe the CN under the effect of a transverse magnetic field, and we discuss the properties of the interaction starting from the unscreened long range Coulomb interaction in two dimensions.

In Section 3 we evaluate the *bulk* and *end* critical exponents. Then we discuss how they are affected by an increasing transverse magnetic field. We remark that α_{bulk} characterizes the discussed power-law behavior of the TDOS, while (α_{end}) characterizes the temperature dependence of G_{max}, in both the UST and the CST regime. Finally, we discuss the presence of an IQD and the magnetic field dependent oscillations in the conductance.

2 Model and interaction

Single particle — Starting from the known bandstructure of graphite, after the definition of the boundary condition (i.e. the wrapping vector $\overrightarrow{w} = (m_w, n_w)$), it is easy to calculate the bandstructure of a CN. For an armchair CN ($m_w = n_w$) we obtain that the energy vanishes for two different values of the longitudinal momentum $\varepsilon_0(\pm K_s) = 0$. After fixing the angular momentum along the y direction to be $m\hbar$, the dispersion law $\varepsilon_0(m,k)$ is usually taken to behave linearly, so that we can approximate it as $\varepsilon_0(m,k) \approx \varepsilon_0(m,K_s) + v_F|k - K_s|$, where we introduce a Fermi velocity v_F (about 10^6 m/s for CNs). In general, we can define an approximated one-dimensional bandstructure for momenta near $\pm K_s = \pm(2\pi)/(3a_0)$

$$\varepsilon_0(m, \overrightarrow{w}, k) \approx \pm \frac{v_F \hbar}{R} \sqrt{\left(\frac{m_w - n_w + 3m}{3}\right)^2 + R^2 \left(k \pm K_s\right)^2} \quad (6)$$

where $R \approx N_b\sqrt{3}a/(2\pi)$ is the tube radius (about 5 nm for MWNTs) and a denotes the honeycomb lattice constant ($a/\sqrt{3} = a_0 = 1.42$ Å).

For a metallic CN (e.g. the armchair one with $m_w = n_w$) we obtain that the energy vanishes for two different values of the longitudinal momentum $\varepsilon_0(\pm K_s) = 0$. The dispersion law $\varepsilon_0(m,k)$ in the case of undoped metallic nanotubes behaves quite linearly near the crossing values $\pm K_s$. The fact of having four low-energy linear branches at the Fermi level introduces a number of different scattering channels, depending on the location of the electron modes near the Fermi points.

Starting from equation (6) we can develop a Dirac-like theory for CNs corresponding to the Hamiltonian

$$H_D = v_F \left[\widehat{\alpha}(\hat{L}_z) + \widehat{\beta}\hat{\pi}_y\right], \quad (7)$$

with a solution in the spinorial form $\widehat{\psi}$ where

$$\widehat{\alpha} = \alpha \begin{pmatrix} 0 & i \\ -i & 0 \end{pmatrix} \quad \widehat{\beta} = \begin{pmatrix} 0 & 1 \\ 1 & 0 \end{pmatrix} \quad \widehat{\Psi} = \begin{pmatrix} \psi_\uparrow \\ \psi_\downarrow \end{pmatrix}. \quad (8)$$

Here $\hat{\pi}_y = \hat{p}_y \pm \hbar K_s$, and $\alpha = \frac{1}{R^2}$, and equation (7) can be compared with the one obtained in reference [30].

For a metallic CN, such as the armchair one, the problem in equation (7) has *periodic boundary conditions*, i.e. $\Psi(\varphi + 2\pi, y) = \Psi(\varphi)$; it follows that a factor $e^{im\varphi}$ appears in the wavefunction. For semiconducting CNs ($m_w \neq n_w$) we have to define *quasiperiodic boundary conditions*, i.e. $\Psi(\varphi + 2\pi, y) = \omega\Psi(\varphi)$ [30] corresponding to a factor $e^{i(m+\frac{m_w - n_w}{3}\varphi)}$ in the wavefunction ($m_0 = m_w - n_w$).

A cylindrical carbon nanotube, with the axis along the y direction and B along z, corresponds to

$$H_D = v_F \left[\widehat{\alpha}(\hat{L}_z) + \widehat{\beta}\left(\hat{\pi}_y - \frac{e}{c}\mathbf{A}\right)\right], \tag{9}$$

where we choose the gauge so that the system has a symmetry along the $\hat{y}$ direction,

$$\mathbf{A} = (0, Bx, 0) = (0, BR\cos(\varphi), 0),$$

and we introduce the cyclotron frequency $\omega_c = \frac{eB}{m_e c}$ and the magnetic length $\ell_\omega = \sqrt{\hbar/(m\omega_c)}$.

It is customary to discuss the results in terms of two parameters, one representing the energy scale following from equation (6)

$$\Delta_0 = \frac{\hbar v_F}{R}, \tag{10}$$

and the second one being the scale of the magnetic field

$$\nu \equiv \frac{\pi R^2}{2\pi\ell_\omega^2} = \frac{\pi R^2 B}{\Phi_0} \quad where \quad \Phi_0 = \frac{hc}{e}. \tag{11}$$

Here we can calculate the effects of the magnetic field by diagonalizing equation (9) after introducing the trial functions,

$$\widetilde{\psi}_{s,m,k}(\varphi, y) = N e^{i(ky + (m+m_0)\varphi)} \times (\alpha_s + \beta_s \sin(\varphi) + \gamma_s \cos(\varphi))). \tag{12}$$

Results are reported in Figure 1 for different CNs and values of the magnetic field.

From the expression of $|\Psi_{m,\pm k}(\varphi, y)|^2$ we deduce a kind of "edge localization" of the opposite current, analogous to the one obtained for the QW [1], also for CNs.

Following the calculations reported in reference [30] for a metallic CN we can easily calculate the linear dispersion relation changes near the band center $\epsilon = 0$. Thus the magnetic field-dependent energy can be written, near the Fermi points $k \sim K_s$, in terms of ν as

$$\epsilon(|k - K_s|) = \pm\hbar|k - K_s|\left(\frac{v_F}{I_0(4\nu)}\right). \tag{13}$$

This describes a reduction of the Fermi velocity $\hbar^{-1}d\epsilon/dk$ near $\epsilon = 0$ by a factor $I_0(4\nu)$.

Hence, the magnetic field-dependent Fermi wavevector follows

$$k_F(\varepsilon_F, \nu, 0) \approx K_s + \left(\frac{\varepsilon_F}{\hbar v_F}\right) I_0(4\nu),$$

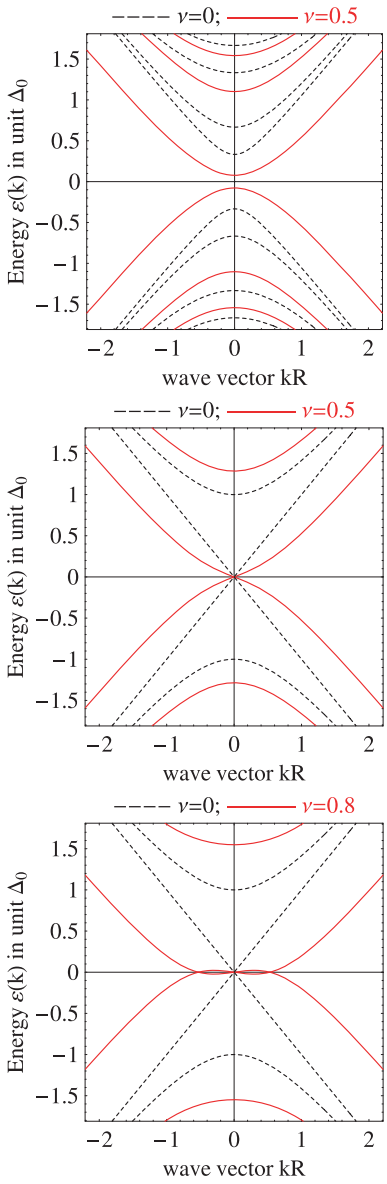

Fig. 1. In the x-axis the wavevector in unit $(k_y - K_s)R$ ($\pi_y R/\hbar$). (Top) Bandstructure of a non-metallic CN with (red lines) and without (black dashed lines) the transverse magnetic field ($\nu = 0.5$). The main consequence of B is the reduction of the semiconducting gap. (Middle and bottom) Bandstructure of a metallic CN with (red lines) and without (black dashed lines) the transverse magnetic field. The main consequence of B at intermediate fields is the rescaling of the Fermi velocity, while for quite strong fields a flat zone appears near $\pi_y = 0$. We know that the magnetic parameter $\nu \approx 0.2$ for $B \sim 5$ T and $R \approx 50$ nm [31].

where the second term in the r.h.s. depends on B as

$$k_F = K_s \pm k_0 + k(B) \approx K_s \pm k_0 \times (1 + 4\nu^2 + ...) \rightarrow k(B) \sim 4k_0\nu^2,$$

where $k_0 = (\frac{\varepsilon_F}{\hbar v_F})$.

Electron-electron interaction — In order to analyze in detail the role of the electron-electron interaction, we

have to point out that quasi 1D devices have low-energy branches, at the Fermi level, which introduce a number of different scattering channels, depending on the location of the electron modes near the Fermi points. It has been often discussed that processes which change the chirality of the modes, as well as processes with large momentum-transfer (known as backscattering and Umklapp processes), are largely subdominant, with respect to those between currents of like chirality (known as forward scattering processes) [32–34]. This hierarchy of the couplings characterizes the Luttinger regime. However, in some special cases the processes neglected here can be quite relevant, also by giving rise to a breakdown of the Luttinger Liquid behaviour [35].

Now, following Egger and Gogolin [34], we introduce the unscreened Coulomb interaction in two dimensions

$$U(\mathbf{r}-\mathbf{r}') = \frac{c_0}{\sqrt{(y-y')^2 + 4R^2\sin^2(\frac{\varphi-\varphi'}{2})}}. \qquad (14)$$

Then, we can calculate $U_0(q,\omega_c)$ starting from the eigenfunctions $\widetilde{\Psi}_{0,k_F}(\varphi,y)$ and the potential in equation (14). We focus our attention on the forward scattering (FS) terms. We can obtain g_2, FS between opposite branches, corresponding to the interaction between electrons with opposite momenta, $\pm k_F$, with a small momentum transfer $\sim q_c$. The strength of this term reads

$$\begin{aligned} g_2 &= U_0(q_c, B, k_F, -k_F) \\ &= \frac{c_0}{N_2(\nu)}\left[K_0\left(\frac{q_cR}{2}\right)I_0\left(\frac{q_cR}{2}\right)\right. \\ &\quad \left. + u_2(\nu)K_1\left(\frac{q_cR}{2}\right)I_1\left(\frac{q_cR}{2}\right)\right], \end{aligned}$$

where $K_n(q)$ denotes the modified Bessel function of the second kind, $I_n(q)$ is the modified Bessel function of the first kind, While N_2 and u_2 are functions of the transverse magnetic field, as we discuss in appendix. Analogously

$$\begin{aligned} g_4 &= U_0(q_c, B, k_F, k_F) \\ &= \frac{c_0}{N_4(\nu)}\left[K_0\left(\frac{q_cR}{2}\right)I_0\left(\frac{q_cR}{2}\right)\right. \\ &\quad \left. + u_4(\nu)K_1\left(\frac{q_cR}{2}\right)I_1\left(\frac{q_cR}{2}\right)\right]. \end{aligned}$$

3 Results

The bulk and the end critical exponents — The first result of this paper concerns the dependence of the critical exponents on the magnetic field, in large radius CNs. By introducing into equation (4) the calculated values of g_2 and g_4, it follows that the bulk critical exponent is reduced by the presence of a magnetic field, as we show in Figure 2.

This prediction can be extended to α_{end}, calculated following equation (5), as we show in Figure 2. Hence, it follows that the exponent $\gamma_e - 1$ can cross from positive to negative values, when the magnetic field increases.

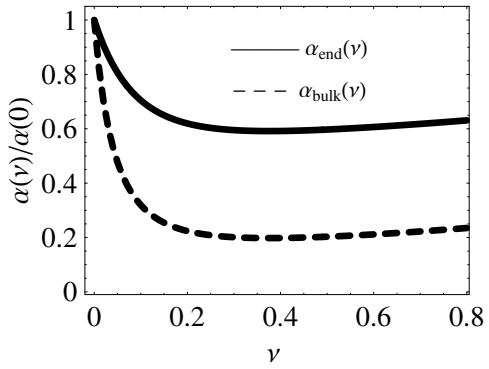

Fig. 2. Critical exponents versus the magnetic field dependent parameter, ν, for a large radius CN: α_{bulk} is calculated following equation (4), α_{end} is calculated following equation (5). The magnetic field rescales the values of the Fermi velocity and the strength of electron-electron interaction. It follows that the effects of a transverse magnetic field also involve the value of K. Thus, we predict a reduction of the critical exponents α_{bulk} and α_{end}, yielding magnetic field-dependent exponents for the power law behaviour of the conductance.

The experimental data about SWNT [7] gives, for vanishing magnetic field, $K_1 \approx 0.26$, $\alpha_{Bulk} \approx 0.27$ and $\alpha_{end} \approx 0.72$.

For a MWNT we consider $N_s \sim 5$ [28,38] so that $K_5 \approx 0.1$, $\alpha_{Bulk} \approx 0.2$ and $\alpha_{end} \approx 0.4$–0.5.

The intrinsic Quantum Dot — When there are some obstacles to the free path of the electrons along a 1D device, a scattering potential has to be introduced in the theoretical model. The presence of two barriers along a CN [7] at a distance d can be represented by a potential

$$V_B(y) = U_B\left(f\left(y+\frac{d}{2}\right) + f\left(y-\frac{d}{2}\right)\right),$$

where $f(y)$ is a square barrier function, a Dirac Delta function or any other function localized near $y=0$.

In order to discuss the presence of magnetic field-dependent oscillations we analyze the transmission in the presence of a magnetic field, $t(\varepsilon_F, B)$, computed for non-interacting electrons, by identifying the off-resonance condition ($|t| = t_{min}$), where electrons are strongly backscattered by the barriers, and the on-resonance condition ($|t| = t_{max}$), where the scattering at low temperatures can be negligible.

Hence, as shown in Figure 3 (top), where we report the transmission $T = |t|^2$ versus ν for the lowest subband, a magnetic field-dependent transmission follows; thus, a magnetic dependence of the peaks in the transmission is shown, which exhibits a magnetically tuned transport through the CN. In particular, assuming that there are two identical, weakly scattering barriers at a distance d, the transmission, computed for non-interacting electrons, is non-zero for particular values of k_F, i.e. those satisying to the condition $\cos(k_F d) \approx 0$. In addition, as it is known (see e.g. Ref. [5]), the system can exhibit a perfect resonant transmission (see Fig. 3, top).

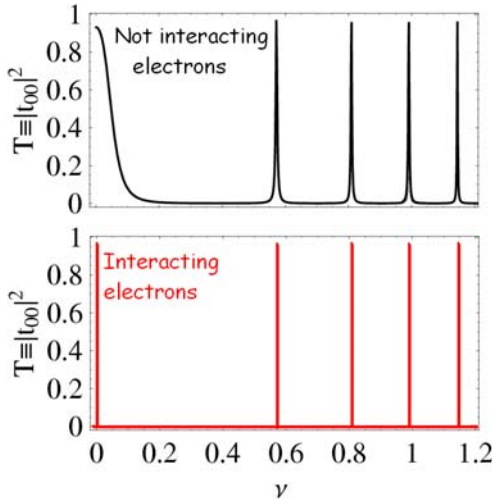

Fig. 3. Transmission (T) of the lowest subband ($m = 0$) as a function of the magnetic field. We use of a double square barrier model, for the IQD. We observe the appearing of resonance peaks, as a function of the magnetic field. The transmission probability was calculated by writing the wavefunctions in each region of the axis y and by imposing the continuity equations at the potential energy discontinuity lines. In the limit of adiabatic transport, thanks to an appropriate projection, the problem of finding the transmission and reflection coefficients can be reduced to an algebraic one. We know that, for quasi one dimensional electron systems, our approach gives results in good agreement with the ones obtained by using some more refined methods, such as the Lippman-Schwinger scattering theory, also in the presence of a magnetic field. The transmission is shown for a non-interacting electron system (top), and is sketched also for an interacting one (bottom), where t is modified by the scaling due to the electron-electron repulsion. The positions of the peaks correspond to those obtained from the condition $\cos(k_F d) \approx 0$, while $0 \leq |t_{00}| \leq 1$, because of the symmetry of the scattering potential.

We consider an IQD with $d \approx 250$ nm in a CN of $R \approx 5$ nm. Thus, starting from the electrons in the middle of the bandgap, i.e. $\varepsilon_F \sim v_F\hbar/(2R)$ $k(B) \approx \nu^2/(2R)$, we have to observe about 4 peaks (the number of resonances with $\nu \leq 1$ is $n_p = d/(4\pi R)$) in the transmission coefficient, when growing the magnetic field from $\nu = 0$ to $\nu = 1$.

The presence of these oscillations could be seen in MWNTs or SWNTs of large radius, while, in the case of a SWNTs with radius $R \approx 1$ nm, the values of the magnetic field are unrealistic. In these systems the effects of the electron-electron interaction cannot be neglected, and they can affect the width and the line shape of the resonances also at zero temperature [5]. It follows that the resonances in the transmission for interacting electrons are of zero width ($w = 0$) and unitary height ($G_{max} = e^2/h$), as in Figure 3 (bottom).

In analogy to our previous paper [1], we can discuss the different explanations of the resonance conditions. From a theoretical point of view, the on-resonance condition can be seen in two different ways: in some papers [36], where the ballistic transport in QWs was analyzed, it was discussed the presence of these peaks as providing evidence of an Aharonov Bohm effect, while in the TLL theory the resonance peaks are put in correspondence to the presence of an average particle number between the two barriers of the form $\nu + 1/2$, with integer ν: thus, we suppose that each electron in the Quantum Dot carries a quantum of magnetic flux.

Temperature behaviour — As it is known, the presence of the peaks in the transmission has to be observable not only at very low temperatures. The temperature does not affect the values of B corresponding to the conductance peaks, while their largest value, G_{max}, follows a power law, according to the Sequential Tunneling theory. Thus, one has $G_{max} \propto T^{\gamma_e - 1}$, with γ_e depending on the tunneling mechanism. This point deserves a brief discussion.

In this paper we take into account a short nanotube section that is created by inducing (e.g. by an atomic force microscope) local barriers into a large radius CN. In this case the condition, $\Delta_{dot} \gg K_B T$ discussed in reference [7] is confirmed in a large range of temperatures around T_R ($\Delta_{dot}/K_B \sim 10^4$ °K, while $\varepsilon_c/K_B \sim 1$ °K).

Now we could discuss the two cases, by assuming the validity of either the UST or the CST. In any case, we want to point out that in both theories, it appears the critical exponent α_{end}, which has to be rescaled with the growing of the magnetic field. It is also known that, when the temperature T is greater than 0, the width of the peaks increases proportionally to T.

The intersubbands processes — The role of the many subbands (N_s) which cross the Fermi level should to be taken into account by introducing the matrix $t_{n,m}$ including all the intersubband scattering processes. However we can suppose $|t_{n,m}| \ll |t_{n,n}|$, corresponding to the adiabatic regime, because the intersubbands processes, i.e. processes that involve two different subbands, are largely subdominant, with respect to processes involving the same subband. It follows that the conductance G results proportional to the sum of the $|t_{n,n}|$. Thus, the peaks corresponding to the on-resonance condition, due to the N_s subbands, have to be superposed, in order to calculate the zero temperature conductance. However, the contribution to the oscillations due to the subbands different from the lowest one can be neglected, because the shift in $k(B)$ is quite smaller for higher subbands, as we show in Figure 1.

4 Conclusions

In this paper we extended to large radius CNs the formalism introduced for a QW in a previous paper. We showed how the presence of a magnetic field modifies the role played by both the electron-electron interaction and the presence of obstacles, in CNs of large radius.

The first prediction that comes from our study is that there should be a significant reduction of the critical exponents, as the magnetic field is increased, in agreement with the results found for QWs.

Our second prediction concerns the presence of some peaks in the beghaviour of the small bias conductance, versus the magnetic field.

$$
\begin{aligned}
U(y-y') &\approx c_0 \int_{-\pi}^{\pi} d\varphi \int_{-\pi}^{\pi} d\varphi' \sqrt{\frac{1}{(y-y')^2+4R^2\sin^2(\frac{\varphi-\varphi'}{2})}} {\Psi^\dagger}_{m,k_F}(\varphi,y)\Psi_{m,k_F}(\varphi,y)\Psi_{n,-k_F}(\varphi',y'){\Psi^\dagger}_{n,-k_F}(\varphi',y') \\
&= \frac{c_0}{4\pi^2}\int_{-\pi}^{\pi} d\varphi \int_{-\pi}^{\pi} d\varphi' \sqrt{\frac{1}{(y-y')^2+4R^2\sin^2(\frac{\varphi-\varphi'}{2})}} \left(\frac{\eta_+ + \theta_+\cos(\varphi') + \xi_+\cos^2(\varphi')}{N_+}\right)\left(\frac{\eta_- + \theta_-\cos(\varphi) + \xi_-\cos^2(\varphi)}{N_-}\right) \\
&\approx \frac{c_0}{4\pi^2}\sqrt{\frac{1}{(y-y')^2}}\int_{-\pi}^{\pi} d\varphi \int_{-\pi}^{\pi} d\varphi' \left(\sum_k^{\infty} \frac{(-1)^k\,\Gamma(\frac{1}{2}+k)}{\sqrt{\pi}\,\Gamma(1+k)}\left(\frac{2R}{y-y'}\right)^{2k}\sin^{2k}\left(\frac{\varphi-\varphi'}{2}\right)\right) \\
&\quad\times\left(\frac{(\eta_+\eta_- + (\eta_+\theta_- + \eta_-\theta_+)\,\cos(\varphi)\,\cos(\varphi') + (\xi_+\cos^2(\varphi) + \xi_-\cos^2(\varphi')))}{(N_+N_-)}\right) \\
&= \frac{2c_0}{N_+N_-}\sqrt{\frac{1}{(y-y')^2}}\sum_n^{\infty}\frac{(-1)^n\,\Gamma(\frac{1}{2}+n)}{\sqrt{\pi}\,\Gamma(1+n)}\left(\frac{2R}{y-y'}\right)^{2n} \\
&\quad\times\left(\left(\eta_+\eta_+ + \frac{\xi_+ + \xi_-}{2}\right)\frac{4\pi^{3/2}\Gamma(n+1/2)}{\Gamma(n+1)} + (\eta_+\theta_- + \eta_-\theta_+)\frac{2\pi^{3/2}n\Gamma(n+1/2)}{\Gamma(n+2)}\right). \qquad \text{(A.1)}
\end{aligned}
$$

It would be of considerable importance to test this behaviour in experiments carried out using different samples, in various temperature regimes. This experimental test can be also useful, in order to solve a controversial question about the exponent that characterizes the power law dependence of $G(T)$.

We want to remark that our approach is based on the idea that electrons tunnel coherently through an obstacle, represented by a double barrier, that can be assumed only as a strong barrier.

Our results could be surely affected by the use of a model, where the electrons weakly interact with the lattice, while the buckles are represented by strong potential barriers. This approximation holds in the opposite regime, with respect to the model of spinless fermions on the lattice used in reference [18]. However, we believe that our model can well reproduce some experimental results while, for what concerns the different regimes, we want also to suggest that, when the temperature decreases, different approaches could be needed, as we discussed in some of our previous papers [37,38].

Appendix A: From the 2D Coulomb potential to a 1D model

First we introduce the wavefunctions Ψ for a metallic CN as spinors constructed starting from the functions

$$\widetilde{\psi}_{s,m,k}(\varphi,y) = \frac{e^{i(ky+im\varphi)}}{N}\left(\alpha_s + \beta_s\sin(\varphi) + \gamma_s\cos(\varphi)\right),$$

it follows

$$
\begin{aligned}
\Psi^\dagger\Psi = \Bigg(\sum_{s=\uparrow,\downarrow}\Big((\alpha_s^2+\beta_s^2) + 2(\alpha_s\gamma_s)\cos(\varphi) \\
+ (\gamma_s^2-\beta_s^2)\cos(\varphi)^2 + [2(\alpha_s\beta_s)\sin(\varphi) \\
+ (\beta_s\gamma_s)\sin(2\varphi)]\Big)\Bigg) \Bigg/ \left(2\pi^2 L\sum_{s=\uparrow,\downarrow}(2\alpha_s^2+\beta_s^2+\gamma_s^2)\right),
\end{aligned}
$$

and we define $\eta_\pm = \sum_{s=\uparrow,\downarrow}(\alpha_s^2+\beta_s^2)$, $\theta_\pm = \sum_{s=\uparrow,\downarrow}2(\alpha_s\gamma_s)$, $\xi_\pm = \sum_{s=\uparrow,\downarrow}(\gamma_s^2-\beta_s^2)$ and $N_\pm = \sum_{s=\uparrow,\downarrow}(2\alpha_s^2+\beta_s^2+\gamma_s^2)$, where $\pm$ corresponds to the values of $k=\pm k_F$.

Now we introduce the Coulomb interaction and expand this function in terms of $R/|y-y'|$ as

$$
\begin{aligned}
U(\mathbf{r}-\mathbf{r}') = \frac{c_0}{|y-y'|}\Bigg(\sum_k^{\infty}\frac{(-1)^k\,\Gamma(\frac{1}{2}+k)}{\sqrt{\pi}\Gamma(1+k)} \\
\times\left(\frac{2R}{y-y'}\right)^{2k}\sin^{2k}\left(\frac{\varphi-\varphi'}{2}\right)\Bigg).
\end{aligned}
$$

The Forward scattering between opposite branches ($\pm$) is obtained as

see equation (A.1) above.

Thus we introduce $u_0 = \eta_+\eta_-$,$u_1 = (\eta_+\theta_- + \eta_-\theta_+)$ and $u_2 = (\xi_+ + \xi_-)$ so that we obtain:

$$
\begin{aligned}
U(y-y') = 2\frac{c_0}{(N_+N_-)}\sqrt{\frac{1}{(y-y')^2}} \\
\times\left\{\left(u_0+\frac{u_1}{2}\right)K\left(-\left(\frac{2R}{y-y'}\right)^2\right)\right. \\
\left.+u_2\left(\frac{\pi}{8}\,{}_2F_1\left(\frac{3}{2},\frac{3}{2};2,-\left(\frac{2R}{y-y'}\right)^2\right)\left[\frac{2R}{y-y'}\right]^2\right)\right\} \qquad \text{(A.2)}
\end{aligned}
$$

where $K_E(x)$ gives the complete elliptic integral of the first kind while ${}_2F_1(a,b,c,z)$ is the hypergeometric function.

The Fourier Transform gives the $U_0(q)$ as

$$
\begin{aligned}
U_0(q) = \frac{c_0}{\sqrt{2}\,(N_+N_-)^2}\Bigg[\left(u_0+\frac{u_1}{2}\right)K_0\left(\frac{qR}{2}\right)I_0\left(\frac{qR}{2}\right) \\
+\frac{u_2}{2}K_1\left(\frac{qR}{2}\right)I_1\left(\frac{qR}{2}\right)\Bigg], \qquad \text{(A.3)}
\end{aligned}
$$

with $K_n(q)$ which gives the modified Bessel function of the second kind and $I_n(q)$ gives gives the modified Bessel function of the first kind.

In order to calculate g_4 we have to define $u_0 = \eta_+^2$,$u_1 = 2\eta_+\theta_+$ and $u_2 = 2\xi_+$ and replace in the equations above.

References

1. S. Bellucci, P. Onorato, Eur. Phys. J. B **47**, 385 (2005)
2. S. Tomonaga, Prog. Theor. Phys. **5**, 544 (1950); J.M. Luttinger, J. Math. Phys. **4**, 1154 (1963); D.C. Mattis, E.H. Lieb, J. Math. Phys. **6**, 304 (1965)
3. A. Yacoby, H.L. Stormer, N.S. Wingreen, L.N. Pfeiffer, K.W. Baldwin, K.W. West, Phys. Rev. Lett. **77**, 4612 (1996); O.M. Auslaender, A. Yacoby, R. de Picciotto, K.W. Baldwin, L.N. Pfeiffer, K.W. West, Phys. Rev. Lett. **84**, 1764 (2000)
4. S.J. Tans, M.H. Devoret, H. Dai, A. Thess, R.E. Smalley, L.J. Geerligs, C. Dekker, Nature **386**, 474 (1997); Z. Yao, H.W.J. Postma, L. Balents, C. Dekker, Nature **402**, 273 (1999)
5. C.L. Kane, M.P.A. Fisher, Phys. Rev. Lett. **68**, 1220 (1992); C.L. Kane, M.P.A. Fisher, Phys. Rev. B **46**, R7268 (1992)
6. H.J. Schulz, e-print `arXiv:cond-mat/9503150`
7. H.W.Ch. Postma, T. Teepen, Z. Yao, M. Grifoni, C. Dekker, Science **293**, 76 (2001)
8. D. Bozovic, M. Bockrath, J.H. Hafner, C.M. Lieber, H. Park, M. Tinkham, Appl. Phys. Lett. **78**, 3693 (2001)
9. M. Sassetti, F. Napoli, U. Weiss, Phys. Rev. B **52**, 11213 (1995)
10. A. Furusaki, Phys. Rev. B **57**, 7141 (1998)
11. A. Braggio, M. Grifoni, M. Sassetti, F. Napoli, Europhys. Lett. **50**, 236 (2000)
12. M. Thorwart, M. Grifoni, G. Cuniberti, H.W.Ch. Postma, C. Dekker, Phys. Rev. Lett. **89**, 196402 (2002)
13. Yu.V. Nazarov, L.I. Glazman, Phys. Rev. Lett. **91**, 126804 (2003)
14. D.G. Polyakov, I.V. Gornyi, Phys. Rev. B **68**, 035421 (2003)
15. A. Komnik, A.O. Gogolin, Phys. Rev. Lett. **90**, 246403 (2003)
16. S. Hügle, R. Egger, Europhys. Lett. **66**, 565 (2004)
17. A. Furusaki, N. Nagaosa, Phys. Rev. B **47**, 3827 (1993)
18. V. Meden, T. Enss, S. Andergassen, W. Metzner, K. Schönhammer, Phys. Rev. B **71**, 041302(R) (2005)
19. J.W. Mintmire, B.I. Dunlap, C.T. White, Phys. Rev. Lett. **68**, 631 (1992); N. Hamada, S. Sawada, A. Oshiyama, Phys. Rev. Lett. **68**, 1579 (1992); R. Saito, M. Fujita, G. Dresselhaus, M.S. Dresselhaus, Appl. Phys. Lett. **60**, 2204 (1992)
20. M. Krüger, M.R. Buitelaar, T. Nussbaumer, C. Schönenberger, L. Forró, Appl. Phys. Lett. **78**, 1291 (2001)
21. S. Bellucci, J. González, Eur. Phys. J. B **18**, 3 (2000); S. Bellucci, *Path Integrals from peV to TeV*, edited by R. Casalbuoni et al. (World Scientific, Singapore, 1999), p. 363, `arXiv:hep-th/9810181`; S. Bellucci, J. González, Phys. Rev. B **64**, 201106(R) (2001); S. Bellucci, J. González, P. Onorato, Nucl. Phys. B **663**, [FS], 605 (2003); S. Bellucci, J. González, P. Onorato, Phys. Rev. B **69**, 085404 (2004)
22. S. Bellucci, P. Onorato, Eur. Phys. J. B **45**, 87 (2005)
23. R. Egger, Phys. Rev. Lett. **83**, 5547 (1999)
24. A. Bachtold, M. de Jonge, K. Grove-Rasmussen, P.L. McEuen, M. Buitelaar, C. Schænenberger, Phys. Rev. Lett. **87**, 166801 (2001); A. Bachtold, M. de Jonge, K. Grove-Rasmussen, P.L. McEuen, M. Buitelaar, C. Schonenberger, report `arXiv:cond-mat/0012262`
25. Z. Yao, H.W.Ch. Postma, L. Balents, C. Dekker, Nature **402**, 273 (1999)
26. H. Ajiki, T. Ando, J. Phys. Soc. Jpn **62**, 1255 (1993)
27. A. Kanda et al., Physica B **323**, 107 (2002)
28. A. Kanda, K. Tsukagoshi, Y. Aoyagi, Y. Ootuka, Phys. Rev. Lett. **92**, 36801 (2004)
29. S. Bellucci, P. Onorato, Annals of Physics **321**, 934 (2006)
30. H.-W. Lee, D.S. Novikov, Phys. Rev. B **68**, 155402 (2003)
31. T. Ando, T. Seri, J. Phys. Soc. Jpn **66**, 3558 (1997)
32. L. Balents, M.P.A. Fisher, Phys. Rev. B **55**, R11973 (1997)
33. R. Egger, A.O. Gogolin, Phys. Rev. Lett. **79**, 5082 (1997)
34. R. Egger, A.O. Gogolin, Eur. Phys. J. B **3**, 281 (1998)
35. S. Bellucci, M. Cini, P. Onorato, E. Perfetto, J. Phys.: Condens. Matter **18**, S2115 (2006)
36. B.J. van Wees, H. van Houten, C.W.J. Beenakker, J.G. Williamson, L.P. Kouwenhoven, D. van der Marel, C.T. Foxon, Phys. Rev. Lett. **60**, 848 (1988)
37. S. Bellucci, P. Onorato, Phys. Rev. B **71**, 075418 (2005)
38. S. Bellucci, J. González, P. Onorato, Phys. Rev. Lett. **95**, 186403 (2005)